Design and optimization of a safflower filament cyclone collection device based on CFD-DEM coupling method

Bangbang Chen[1], Xiangdong Liu[1*], Xuzhe Sun[1], Kejia Zhuang[2], Dongyun Wang[3], Baojian Ma[1*]

(1. *School of Mechatronic Engineering, Xinjiang Institute of Technology, Aksu 843100, Xinjiang, China*;
2. *School of Mechanical Electronic Engineering, Wuhan University of Technology, Wuhan 430070, China*;
3. *College of Engineering, Zhejiang Normal University, Jinhua 321004, Zhejiang, China*)

Abstract: To address the bottleneck problems of low collection efficiency and high impurity content in the mechanical harvesting of safflower filaments, this study takes Xinjiang dryland safflower as the research object and designs an efficient cleaning system for safflower filaments based on the cyclone separation principle. To optimize system performance, this study integrates Computational Fluid Dynamics and Discrete Element Method (CFD-DEM) coupled simulations with the Response Surface Methodology (RSM), systematically investigating the effects of three key parameters—volute wrap angle, separation drum diameter, and inlet air velocity—on cleaning performance. Through coupled simulations, the internal flow field characteristics (indicated by pressure drop and resultant velocity) and the movement trajectories of the filaments were thoroughly analyzed. Based on a three-factor, three-level response surface experimental design, accurate regression models for the collection rate and impurity rate of the filaments were established, and the interactive effects among the parameters were revealed. Optimization results show that under the optimal parameter combination of a 180° volute wrap angle, 140 mm separation drum diameter, and 2.5 m/s inlet air velocity, the cleaning performance is optimal, with a measured filament collection rate of 98.53% and an impurity rate of 2.30%, which are in close agreement with the model predictions (relative error <5%). This study not only verifies the effectiveness and accuracy of the CFD-DEM coupled method in the design of agricultural material cleaning equipment but also provides a reliable theoretical basis and technical solution for the efficient and low-loss mechanical harvesting of safflower filaments.

Keywords: safflower filaments, CFD-DEM, cyclone collector, parameter optimization
DOI: 10.25165/j.ijabe.20261904.10274

Citation: Chen B B, Liu X D, Sun X Z, Zhuang K J, Wang D Y, Ma B J. Design and optimization of a safflower filament cyclone collection device based on CFD-DEM coupling method. Int J Agric & Biol Eng, 2026; 19(4): 67–78.

1 Introduction

Safflower (*Carthamus tinctorius* L.), a versatile economic crop, serves as a source of medicine, dye, oil, and fodder[1,2]. The comprehensive utilization of its filaments, fruits, stems, and leaves has garnered significant attention. With the rapid development of the safflower industry, particularly driven by industrialization and commercialization, its role in social and regional economies is becoming increasingly important. However, within the safflower industry chain, the harvesting of filaments still relies predominantly on manual labor, leading to issues such as high labor intensity and low picking efficiency. Although some mechanical picking devices have been introduced, achieving efficient and low-loss collection of safflower filaments remains a challenging problem to solve[3]. Consequently, developing mechanized harvesting technology suitable for safflower filaments holds substantial theoretical and practical significance.

The mechanized harvesting process of safflower primarily involves two key stages: the separation of filaments from the seed head, and the collection of the separated filaments. While some related research has been conducted by domestic and international scholars in recent years, existing mechanized harvesting equipment still faces technical bottlenecks and has not yet seen widespread application. For instance, Zhang et al.[4] designed an arc-progressive safflower filament harvesting device that uses rotating blades to cut the filaments, achieving low-damage picking. Zhang et al.[5] developed a safflower picking robot integrated with image recognition technology, capable of precisely locating picking positions. However, compared to the high mechanization level of flower separation, filament collection remains a difficulty in the harvesting process. Other scholars have made attempts; for example, Cao et al.[6] designed a comb-clamp picking device that secures the seed head through timed actions and collects filaments via negative pressure, but issues persist regarding high filament damage rates and difficulty in meeting impurity rate requirements. An et al.[7] designed an intelligent harvesting platform capable of picking and collecting filaments but did not deeply explore the working conditions of the negative pressure fan or effectively address the problem of filament cleaning.

In the field of cleaning and collecting agricultural materials, air-and-screen cleaning and pneumatic separation are mainstream technologies. The former combines airflow and vibrating screens to separate materials, while the latter utilizes airflow to separate

Received date: 2025-10-22 **Accepted date:** 2026-06-11
Biographies: Bangbang Chen, PhD, Associate Professor, research interest: intelligent agricultural machinery. Email: chenbangbang@st.xatu.edu.cn; **Xuzhe Sun**, Engineer, research interest: agriculture machinery. Email: ynyx21@126.com; **Kejia Zhuang**, PhD, Professor, research interest: agriculture machinery. Email: zhuangkj@whut.edu.cn; **Dongyun Wang**, PhD, Professor, research interest: agricultural robot. Email: zsdwdy@zjnu.edu.cn.
***Corresponding author: Xiangdong Liu**, PhD, Professor, research interest: intelligent agricultural machinery. School of Mechatronic Engineering, Xinjiang Institute of Technology, Aksu 843100, Xinjiang, China. Tel: +86-16699271569, Email: iceast@foxmail.com; **Baojian Ma**, PhD, Associate Professor, research interest: agricultural robot. School of Mechatronic Engineering, Xinjiang Institute of Technology, Aksu 843100, Xinjiang, China. Tel: +86-17788594899, Email: 11813019@zju.edu.cn.

materials based on their characteristics[8]. In recent years, pneumatic separation technology has gradually been applied in crop collection and cleaning, with significant attention given to the separation efficiency of particulate materials. For example, Liao et al.[9] introduced cyclone separation technology into the cleaning device of rapeseed combine harvesters, significantly reducing impurity content. Huang et al.[10] optimized the performance of a buckwheat cyclone separation cleaning device through CFD-DEM simulation, effectively improving cleaning efficiency and purity. The coupled simulation technology of Computational Fluid Dynamics (CFD) and the Discrete Element Method (DEM) has become a powerful tool for in-depth study of the complex gas-solid two-phase flow field and particle motion patterns inside separators, enabling precise optimization[11-13].

To understand the patterns of airflow and particle motion, scientists have employed various research methods, such as experimental analysis and theoretical/empirical equation methods. Although each research method for cyclone separators can achieve their design and optimization, many researchers opt for optimization through CFD numerical simulation. For instance, Juengcharoensukying et al.[14] studied the influence of cyclone separator and inlet angle on separation performance using CFD numerical simulation.

With the continuous refinement of cyclone separation technology, scholars have successfully applied this technology to optimize devices such as a maize seed meter[15] and a calcium fruit cleaning and collection device[16]. Wasilewski et al.[17] enhanced separation efficiency by introducing a vortex finder to strengthen airflow turbulence effects but did not consider the impact of material characteristics on its performance. Huang et al.[18] used CFD two-way coupling technology to establish a coupling model between material feed rate and separation efficiency, revealing the influence of feed rate on the operational performance of the cyclone separator, but did not integrate real-time control technology. Li et al.[19] developed a roller-rubbing cylindrical screen cleaning device suitable for high-moisture millet, achieving certain breakthroughs in cleaning accuracy, but its structure is complex and maintenance costs are high. Wang et al.[20] designed a wind selection collection device for ratoon rice using a six-blade centrifugal fan combined with CFD software simulation. Hou et al.[21] addressed the lack of dedicated cleaning collection devices for castor harvesting by designing a double-layer inclined vibrating air-and-screen cleaning device, with bench tests verifying a practical screening efficiency of 93.15%, but its loss rate (6.94%) and vibration energy consumption were high. Theoretical analysis and preliminary experiments indicate that the physical characteristics (such as particle size and density) of safflower filaments and their impurities are comparable to those of the aforementioned crops, suggesting the potential for efficient collection and cleaning.

In summary, to address the core bottlenecks of “difficult collection and high impurity content” in safflower filament harvesting, this study innovatively proposes a scheme for designing a cyclone collection system for safflower filaments based on the CFD-DEM coupling method. Its main contributions include: 1) Designing a dedicated cyclone separation cleaning and collection device for safflower filaments based on gas-solid two-phase flow theory; 2) Systematically studying the influence of key structural parameters (such as volute wrap angle and separation drum diameter) and operational parameters of the cyclone collector on collection performance using the CFD-DEM coupled simulation method, and performing parameter optimization; 3) Further validating the actual collection performance of the optimized device through bench tests, providing a reliable theoretical basis and key technical support for the efficient and low-loss harvesting of safflower filaments.

2 Structure of the safflower filament cyclone collection system

The structure of the safflower filament cyclone collection system is shown in Figure 1. It mainly consists of an end-effector, a conveying hose, a cyclone collector, a negative pressure fan, and a collection box.

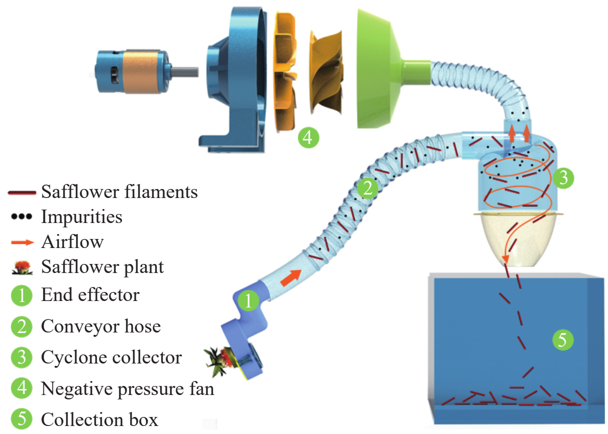

Figure 1 Safflower filament cyclone collection system

During harvesting operations, the vision perception and decision-making control system guides the robotic arm to position the picking end-effector at the target location. The negative pressure airflow generated by the fan draws the filaments into the contoured gathering inlet. Under the cutting action of the bionic blades, the filaments are separated from the seed head. The separated filaments enter the cyclone collector via the conveying hose. Under the combined action of centrifugal force and airflow, the filaments move along the inner wall of the collector and slide down into the collection box, achieving non-damaging separation and collection. Throughout the collection process, the cyclone collector is the core component of the system. Therefore, the subsequent research focuses on the design and optimization of the cyclone collector based on the material characteristics of safflower filaments.

3 Design of the safflower filament cyclone collector

Based on the working principle of the end-effector and the cyclone separation principle, the negative pressure airflow must adsorb the safflower filaments vertically within the end-effector to facilitate cutting by the bionic blades, while the collection device needs to separate the filaments from the air. Therefore, during the safflower harvesting process, the airflow rate of the negative pressure device directly determines the harvesting effectiveness of both the end-effector and the collection device, making it necessary to calculate and analyze its flow rate. To ensure the negative pressure within the end-effector meets the requirements for cutting safflower filaments, and with reference to the fluid kinematic characteristics of agricultural materials, the feed rate q of the separation device was set to 0.03 kg/s. When safflower filaments are fed into the separation drum, assuming only filaments and air are present and are fed uniformly, the airflow rate Q inside the separation drum can be calculated using Equation (1).

$$Q = \frac{q}{\rho_a u_m} \tag{1}$$

where, q is the feed rate of the safflower filament separation system, taken as 0.03 kg/s; u_m is the mass ratio of filaments to the total air-material mixture in the airflow within the separation drum. Referring to the typical concentration values for pneumatic conveying of fibrous agricultural materials, this value is taken as 0.6; ρ_a is the air density, taken as 1.2 kg/m^3. Using Equation (1), the calculated required airflow rate for safflower filament separation is 0.042 m^3/s.

3.1 Analysis of safflower filament suspension velocity

According to the force balance principle and the force analysis on the filament model, the model is subjected to gravity, buoyancy, and drag force in the vertical direction. A correction factor is introduced when solving for the suspension velocity of non-spherical materials. The suspension velocity zonal calculation method and the equivalent particle size method are used to determine the air drag coefficient. Substituting the model parameters and airflow characteristic parameters into the force balance equation yields the suspension velocity of the safflower filaments [22-23]. The specific theory is as follows:

$$G = \rho g r_1 r_2 r_3 \tag{2}$$

$$F_t = \frac{1}{2} C_P S v_f^2 \tag{3}$$

$$G = F_a + F_t \tag{4}$$

$$S = r_1 r_2 \tag{5}$$

The suspension velocity equation can be derived and calculated from Equations (2)-(5), as shown in Equation (6):

$$v_f = \sqrt{\frac{2 g r_1 (\rho - \rho_a)}{C_p - \rho}} \tag{6}$$

The meanings of the above symbols are explained in Table 1.

Table 1 Parameter definitions

Symbol	Description	Unit
G	Safflower filament weight	N
ρ	Safflower filament density	kg/m^3
g	Gravitational acceleration	m/s^2
r_1	Safflower filament length	m
r_2	Safflower filament width	m
r_3	Safflower filament height	m
F_t	Air buoyancy	N
F_a	Air resistance	N
C_p	Drag coefficient	/
ρ_a	Air density	kg/m^3
S	Suction port area	m^2
v_f	Safflower filament suspension velocity	m/s

Since the drag coefficient C_p is a function of the particle Reynolds number R_e, it is difficult to directly solve for the suspension velocity of the material particle. Therefore, the drag coefficient is determined based on the range of the equivalent diameter of the particle material being tested, with the relationship shown in Equations (7) and (8) [24]:

$$C_p = \begin{cases} \frac{24}{R_e} R_e, & R_e < 0.5 \\ \frac{24(1+0.15R_e^{0.67})}{R_e}, & 0.5 \le R_e < 1000 \\ 0.44, & R_e > 1000 \end{cases} \tag{7}$$

$$R_e = \frac{\rho_a d_v v_f}{\mu} \tag{8}$$

where, μ is the dynamic viscosity of air, Pa·s; d_v is the equivalent diameter, m.

Based on preliminary experiments measuring relevant material characteristic parameters of the safflower filaments, the density was determined to be 650 kg/m^3, and the equivalent diameter d_v was approximately 0.001 66 m. Using an air density ρ_a of 1.2 kg/m^3 and a dynamic viscosity of air μ of 1.82×10^{-5} Pa·s, these parameters were substituted into the equations to determine the corresponding range for the equivalent diameter related to the drag coefficient. The calculated drag coefficient C_p was 0.44, yielding a theoretical free suspension velocity for the safflower filaments in the range of 1.85-3.08 m/s.

3.2 Collector structural parameter design

As shown in Figure 2, the cyclone collector designed in this study mainly consists of a suction inlet, a discharge outlet, a negative pressure outlet, and a plunger tube. The negative pressure outlet is connected to the negative pressure fan via a conveying hose, providing a continuous and stable negative pressure airflow within the system. Based on the distribution characteristics of the airflow velocity inside the drum, the spatial region can be divided into a high-velocity airflow zone and a low-velocity airflow zone: the former is primarily distributed near the central plunger tube, while the latter is concentrated near the inner wall of the drum. After safflower filaments enter the separation drum with the airflow through the suction inlet, they are acted upon by centrifugal force and move downward along a rotational trajectory within the low-velocity airflow zone near the drum's inner wall. As they gradually settle under the influence of gravity and airflow, the filaments detach from the airflow control and fall through the discharge outlet into the collection box when the upward airflow velocity falls below their critical suspension velocity, thereby achieving gas-solid separation and efficient filament recovery. In this process, both the structural parameters of the cyclone collector (such as the drum diameter, plunger tube diameter, and cone angle) and its airflow velocity significantly impact the separation efficiency. Therefore, this section conducts a systematic study on the optimal design of the cyclone collector structure and parameter matching strategies, based on the physical characteristic parameters of safflower filaments.

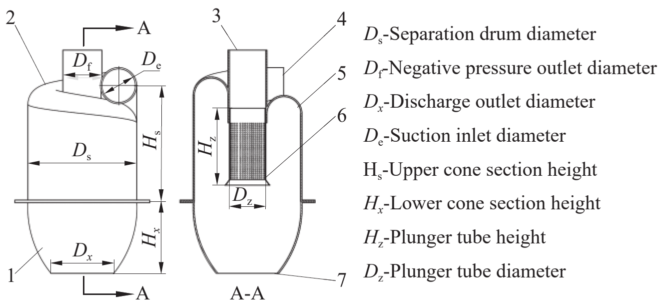

1. Lower cone section 2. Upper cone section 3. Negative pressure outlet 4. Suction inlet 5. Drum inner wall 6. Plunger tube 7. Discharge outlet

Figure 2 Schematic diagram of the collector structure

The dimensional parameters of the collector structure are key factors affecting collection performance. Under a constant airflow rate, if the separation drum diameter is too large, the centrifugal force experienced by the safflower filaments is small, leading to reduced collection efficiency. If the separation drum diameter is too small, the centrifugal force on the filaments increases, potentially causing them to be rebounded towards the high-velocity airflow zone near the plunger tube and subsequently carried into the negative pressure fan with the airflow. Therefore, comprehensively considering the maximum suspension velocity of safflower filaments (3.08 m/s) and the design and installation requirements of the collector structure, the separation drum diameter can be determined using Equation (9).

$$D_s = \sqrt{\frac{4Q}{\pi v_{f\max}}} \tag{9}$$

where, $v_{f\max}$ is the maximum suspension velocity of the safflower filaments, and π is taken as 3.14. Calculation yields $D_s \approx 130$ mm. Considering the overall structural layout of the harvesting system and based on existing design experience for cyclone separation drums and preliminary experimental test data, the design structural parameters for the safflower filament collector were determined as listed in Table 2.

Table 2 Collector structural parameters

Structural parameter	Dimensional relationship	Value/mm
Separation drum diameter (D_s)	D_s	130
Negative pressure outlet diameter (D_f)	(0.2-0.4) D_s	45.5
Discharge outlet diameter (D_x)	0.57 D_s	74.1
Suction inlet diameter (D_e)	(0.2-0.4) D_s	45.5
Upper cone section height (H_s)	0.91 D_s	118.3
Lower cone section height (H_x)	0.73 D_s	94.9
Plunger tube height (H_z)	0.65 D_s	84.5
Plunger tube diameter (D_z)	(0.2-0.4) D_s	45.5

3.3 Optimization of the cyclone collector structure

3.3.1 Optimization model

Based on the safflower filament cyclone collector designed above, the structural parameter of the volute wrap angle at the suction inlet is a crucial factor affecting the separation efficiency of the filaments. This section utilizes fluid simulation via Fluent software (ANSYS Fluent 2022 R1) to investigate the influence of the volute wrap angle and diameter on the velocity profile within the cyclone collector[25], while ensuring the negative pressure at the gathering inlet of the end-effector, in order to determine the optimal structural parameters. The most widely used numerical turbulence models are primarily the Standard *k*-*ε* model, the Renormalization Group (RNG) *k*-*ε* model, and the Reynolds Stress Model (RSM). The Standard *k*-*ε* model, which solves primarily for turbulent kinetic energy (*k*) and turbulent dissipation rate (*ε*), is generally applied to gaseous turbulence models with limited computational resources and simple flows. Using the Standard k-ε model for simulating the strong swirling flow involved in the separation of safflower filaments in this study could lead to significant errors. The RSM solves the Reynolds stress transport equations directly. Compared to the Standard and RNG *k*-*ε* models, the RSM abandons the isotropic eddy viscosity assumption and fully accounts for the anisotropy of turbulence in its calculations. Although this model offers high accuracy, its parameter setup and solution process are more complex, and the computational time is considerably longer. In contrast, the RNG *k*-*ε* model introduces renormalization group theory upon the foundation of the Standard *k*-*ε* model. This model modifies the turbulent eddy viscosity coefficient and incorporates the effect of small-scale eddies on energy transfer, providing better simulation performance for flow fields with transient flows and high streamline curvature. Furthermore, this model requires less computational effort.

Considering the airflow variations within the safflower filament collector and the low mass of the filaments, among other factors, this study adopts the RNG *k*-*ε* model for the numerical simulations. The fundamental equations for this model are as follows:

$$\frac{\partial(\rho k)}{\partial t} + \frac{\partial(\rho u_i k)}{\partial x_i} = \frac{\partial}{\partial x_j}\left(\alpha_k \mu_{eff} \frac{\partial k}{\partial x_j}\right) + G_k - \rho\varepsilon \tag{10}$$

$$\frac{\partial(\rho\varepsilon)}{\partial t} + \frac{\partial(\rho u_i \varepsilon)}{\partial x_i} = \frac{\partial}{\partial x_j}\left(\alpha_\varepsilon \mu_{eff} \frac{\partial \varepsilon}{\partial x_j}\right) + \frac{\varepsilon}{k}\left(C_{1\varepsilon}^{*} G_k - \rho C_{2\varepsilon}\varepsilon\right) \tag{11}$$

where, $\mu_{eff} = \mu + \mu_t$, $\mu_t = \rho C_\mu \frac{k^2}{\varepsilon}$, $C_\mu = 0.0845$, $\alpha_k = \alpha_\varepsilon = 1.39$, $C_{2\varepsilon} = 1.68$, $C_{1\varepsilon}^{*} = 1.42 - \frac{\eta(1-\eta/\eta_0)}{1+\beta\eta^3}$, $\eta = \frac{k}{\varepsilon}\sqrt{2E_{ij}\cdot E_{ij}}$, $E_{ij} = \frac{1}{2}\times\left(\frac{\partial u_i}{\partial x_j} + \frac{\partial u_j}{\partial x_i}\right)$, $\eta_0 = 4.377$, $\beta = 0.012$.

3.3.2 Structural parameter optimization

(1) Simulation analysis of different volute wrap angles

The volute wrap angle is a key parameter affecting the flow field and separation efficiency within the cyclone collection device. This study conducted simulation-based optimization analysis focused on the influence of the volute wrap angle on the airflow characteristics and separation efficiency of the cyclone collector. In Fluent software, four cyclone collectors with different volute wrap angles (90°, 135°, 180°, and 225°) were selected for simulation. The computations were performed on a workstation equipped with an AMD Ryzen Threadripper PRO 3975WX 32-core processor, an NVIDIA RTX A5000 GPU, and 384 GB of RAM (operating at 3.50 GHz). The separation drum diameter was uniformly set at 130 mm, and the suction inlet was defined as a velocity inlet. Based on the free suspension velocity of safflower filaments, the inlet air velocity was set at 2.4 m/s to ensure effective penetration of the airflow through the material while avoiding excessive disruption of the filaments' motion characteristics. As shown in Figure 3, the pressure contours, velocity contours, and particle trajectory plots on the *Y*-*Z* cross-section were simulated for cyclone collectors with different volute wrap angles.

From the simulation results in Figure 3, it can be observed that the resultant velocity within the cyclone collector gradually increases as the volute wrap angle increases. When the volute wrap angle increased from 90° to 225°, the resultant velocity increased from 6.62 m/s to 7.9 m/s. Notably, the velocity increase was more significant during the transition from 90° to 135°, rising to 7.11 m/s. Furthermore, the pressure contours indicate that the pressure differential within the device changed with increasing volute wrap angle. The pressure differential continuously increased as the volute wrap angle increased from 90° to 180°, but the rate of increase diminished when the angle was further increased to 225°.

Further analysis of the particle trajectory plots revealed that at volute wrap angles of 90°, 135°, and 225°, distinct zones of sudden velocity increase existed at the interface between the suction inlet and the internal flow field of the cyclone collector, leading to uneven airflow distribution. This non-uniform velocity distribution is detrimental to flow field stability and may increase the risk of filament breakage due to collisions between filaments and the wall or among themselves. Particularly at the 225° volute wrap angle, the uneven velocity distribution was more severe, consequently preventing the airflow from effectively carrying the filaments to complete the collection task. For volute wrap angles of 135° and 225°, the airflow path was shorter; the airflow exited through the negative pressure outlet without fully passing through the lower part of the collector, thus failing to adequately complete material collection. Therefore, comprehensively considering the negative pressure effect at the suction inlet and the lightweight physical characteristics of safflower filaments, this study preliminarily selected a volute wrap angle of 180° as the optimized design to improve the separation and collection efficiency of the filaments.

(2) Simulation analysis of different separation drum diameters

Regarding the collector separation drum diameter, the calculated value based on Equation (9) was 130 mm. To further optimize the collector structural design, this study selected five separation drum diameters 110 mm, 120 mm, 130 mm, 140 mm, and 150 mm for simulation. All models had a volute wrap angle of 180° and an inlet velocity of 2.4 m/s. The simulation results are shown in Figure 4.

From Figure 4, it can be seen that the pressure differential inside the cyclone collector changes as the separation drum diameter increases. When the diameter increased from 110 mm to 150 mm, the pressure differential initially increased gradually. However, as the diameter continued to increase beyond this range, the pressure differential began to decrease. Changes in the pressure differential directly affect the centrifugal force inside the cyclone collector, consequently influencing the separation efficiency of the safflower filaments and the stability of the equipment. To ensure an efficient safflower filament cleaning process and stability of the internal flow field, a cyclone collector with a larger pressure differential should be selected.

Analysis of the velocity contours on the longitudinal section of cyclone collectors with different diameters shows that the airflow velocity exhibits good symmetry along the central axis of the collector. The velocity is higher at the negative pressure outlet and lower and more uniform near the drum wall. As the separation drum diameter changes, the velocity difference between the negative pressure outlet and the suction inlet gradually increases. The magnitude of this velocity difference directly affects the strength of the centrifugal force. Therefore, to improve the cleaning efficiency of the safflower filaments, a cyclone collector with a larger velocity difference should be selected.

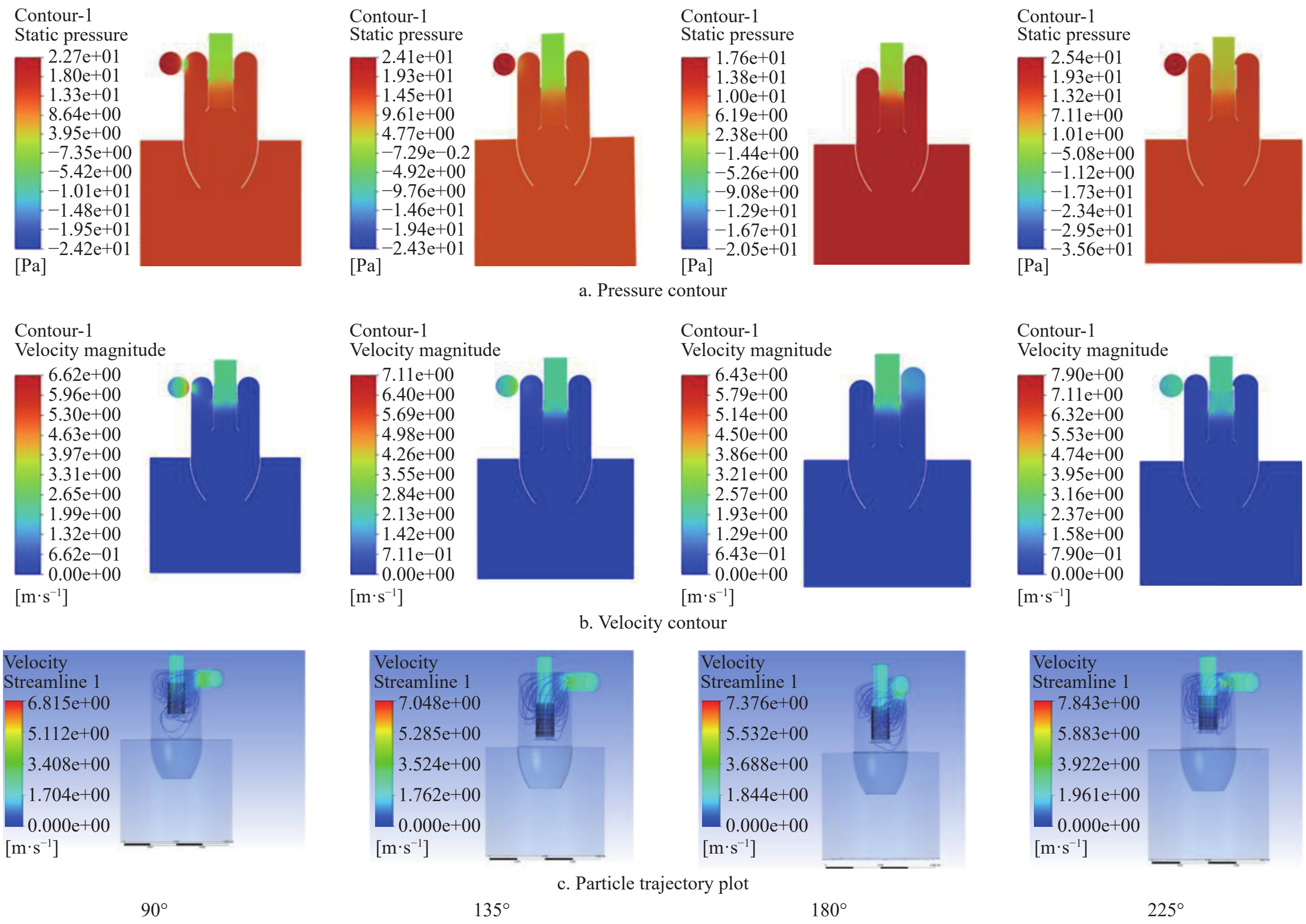

a. Pressure contour

b. Velocity contour

c. Particle trajectory plot

Figure 3 Simulation results for different volute wrap angles

By tracking the airflow and observing the instantaneous motion trajectories of the filaments under different separation drum diameters, it was found that after the airflow enters the cyclone collection device through the suction inlet, it flows along the drum wall around the suction inlet. The filaments are carried into the collection device by the combined action of centrifugal force and gravity, while impurities are carried upward by the airflow and expelled through the negative pressure outlet. Analysis combining the pressure contours and particle tracking plots revealed no observable airflow backflow, and the particle trajectories were stable. Comprehensively considering factors such as pressure drop, resultant velocity, and motion trajectories, the collector with a separation drum diameter of 140 mm was ultimately selected as the optimal design.

In summary, through simulation-based optimization analysis, this study preliminarily determined the cyclone collector design with a 180° volute wrap angle and a 140 mm separation drum diameter as the optimized solution. This configuration demonstrates good separation efficiency and airflow stability, effectively enhancing the collection performance for safflower filaments.

3.4 Optimization and verification of operating parameters for the safflower filament cyclone collector

3.4.1 Negative pressure air velocity parameter optimization

After determining the volute wrap angle and separation drum diameter of the cyclone collection device, gradient comparison experiments were designed to optimize the separation efficiency while ensuring low energy consumption. Using a suction inlet velocity of 2.4 m/s as the mid-point and a variable increment of 0.2 m/s, suction inlet velocity gradient experiments were conducted to determine the optimal operating parameters for the cyclone collection device. The simulation results are shown in Figure 5, displaying the pressure contours, velocity contours, and particle trajectory plots for suction inlet velocities of 2.0 m/s, 2.2 m/s, 2.4 m/s, 2.6 m/s, and 2.8 m/s.

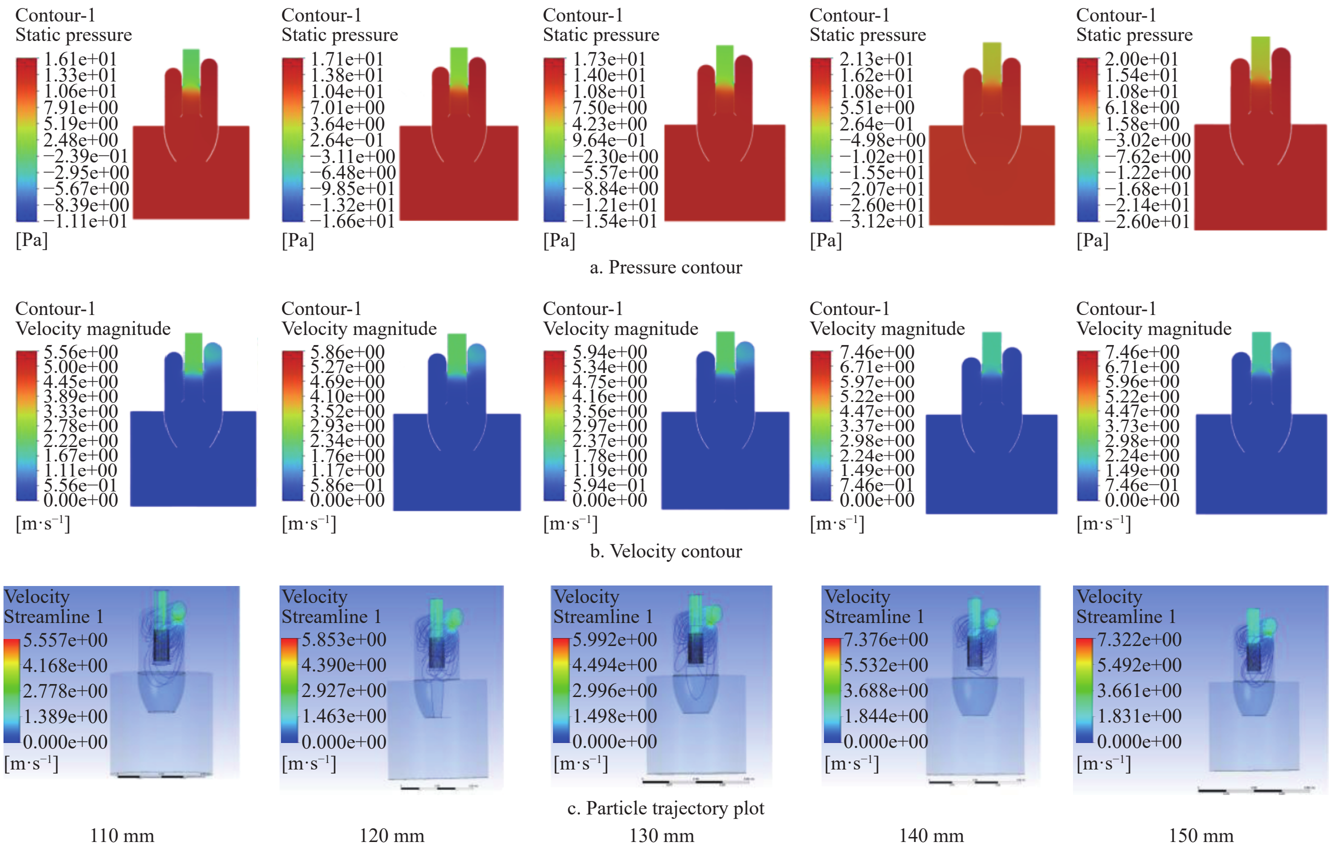

Figure 4 Simulation results for different separation drum diameters

Analysis of the pressure contours indicates that the pressure differential inside the device changes as the suction inlet velocity increases. When the velocity increased from 2.0 m/s to 2.2 m/s, the pressure differential rose. However, when the velocity increased further from 2.2 m/s to 2.4 m/s, the pressure differential decreased slightly. As the suction inlet velocity continued to increase beyond this point, the pressure differential increased again. Results from the velocity contour analysis show that compared to the lower suction inlet velocity settings of 2.0 m/s and 2.2 m/s, velocities of 2.4 m/s, 2.6 m/s, and 2.8 m/s resulted in a more uniform velocity distribution within the flow field. Furthermore, as the suction inlet velocity increased, the resultant velocity increased, thereby enhancing the centrifugal force and improving the separation efficiency of the cyclone collection device. Simulation results from the particle trajectory plots demonstrate that particle trajectories met the functional requirements of the cyclone separation device, namely, the cleaning and collection of safflower filaments under all tested suction inlet velocities. However, with increasing suction inlet velocity, the resultant velocity gradually increased, and the issues of uneven velocity distribution and the area of sudden velocity increase within the cyclone collector expanded, which could affect flow field stability and lead to filament damage.

Comprehensive analysis reveals that as the suction inlet velocity increases, both the internal pressure differential and the resultant velocity of the internal flow field increase, and the area of sudden velocity increase changes continuously, leading to improved separation efficiency. However, due to the increasing flow field velocity unevenness and the excessive centrifugal force caused by the larger pressure differential, the filament damage rate also rises. Balancing energy consumption, separation efficiency, and filament damage rate, this study ultimately determined a suction inlet velocity of 2.4 m/s as the optimal operating condition to maximize separation efficiency while minimizing filament damage.

3.4.2 Performance verification of the cyclone collector based on CFD-DEM

Safflower filaments, as flexible, flaky materials, involve complex force analysis and present research challenges due to their slender and asymmetric shape characteristics. To simplify this process, this study approximated the non-spherical particles as spherical materials using physical parameters such as equivalent diameter, shape parameters, and average density[26]. The established discrete element model of the safflower filament is shown in Figure 6. Fluid computation software (Fluent) and the Discrete Element Method (EDEM 2022, Altair Engineering Inc.) were further employed for data calculation with this model to investigate the performance of the safflower filament separation device under different working conditions and to provide data support for optimized design. Based on preliminary experimental research and relevant literature, the density, Poisson's ratio, and shear modulus of the selected safflower filament material were determined, with detailed parameters listed in Table 3.

To improve computational efficiency, 100 safflower filament models were set up in the EDEM simulation, with a ratio of intact forms to damaged forms of 2:1. To ensure simulation accuracy, contact characteristic parameters between the safflower filaments and the walls of the cyclone separation device were defined, considering the direction of gravitational acceleration. The safflower filament surface was defined as smooth with negligible adhesion. The Hertz-Mindlin (no-slip) contact model was applied for interactions between filaments themselves and between filaments and walls. The material simulation parameters are listed in Table 4.

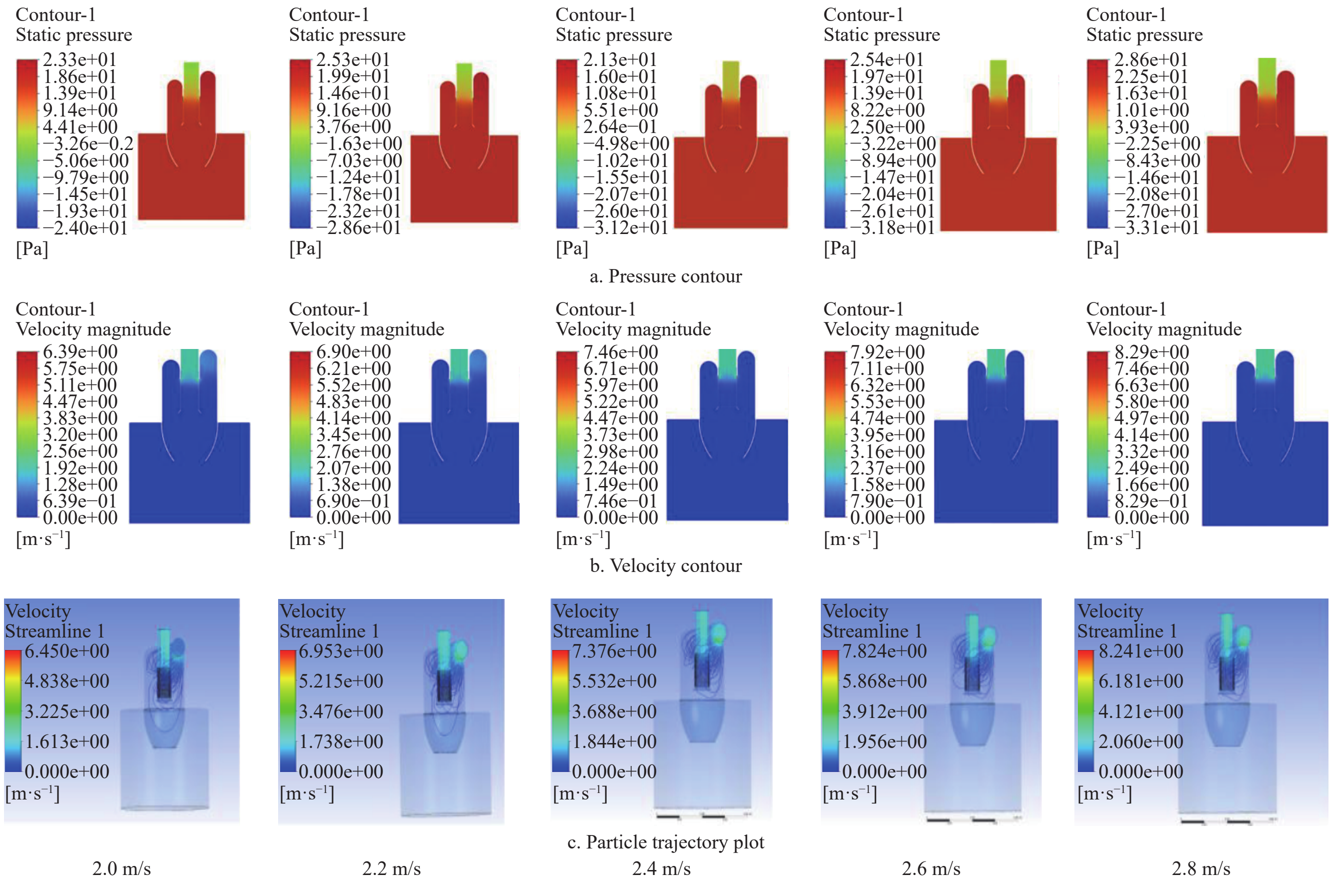

Figure 5 Simulation results for different negative pressure air velocities

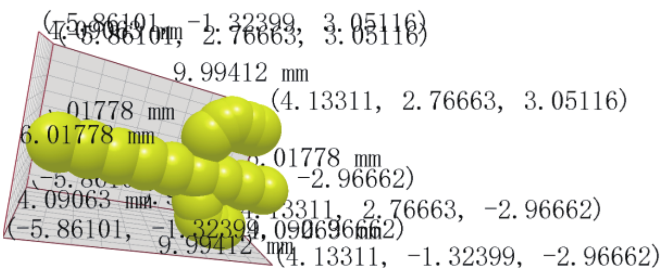

Figure 6 Discrete element model of the safflower filament

Table 3 Material characteristics of safflower filaments

Material	Poisson's ratio	Shear modulus/Pa	Density/kg·m^{-3}
Safflower filament	0.25	1.53×10^{6}	650
Plastic	0.39	2.2×10^{9}	1418

Table 4 Simulation parameters

Material	Coefficient of restitution	Dynamic friction coefficient	Static friction coefficient
Filament-filament	0.6	0.3	0.56
Filament-wall	0.6	0.26	0.7

Through EDEM-Fluent coupled simulation, the motion trajectories of the safflower filaments within the separation device could be visually observed, as shown in Figure 7. The figure shows that the filaments enter the cyclone separation drum through the suction inlet with a certain initial velocity. Under the combined action of gravity and the swirling airflow, the filaments begin to spiral downward along the inner wall of the drum. During this movement, most filaments follow the spiral airflow into the collection box. Only a very small fraction deviates from the spiral airflow path and moves towards the high-velocity airflow zone in the center of the drum, resulting in some filaments adhering to the surface of the central plunger tube. To evaluate the separation efficiency, statistical zones were defined at the suction inlet and the discharge outlet. The damage rate, calculated as the mass difference between filaments at the suction inlet and the discharge outlet relative to the mass at the discharge outlet, was approximately 2.5%.

4 Performance test of the safflower filament cyclone collector

4.1 Test materials and methods

To further optimize and verify the performance of the cyclone collection device, a performance test platform for safflower filament harvesting was established, as shown in Figure 8. This platform

a. Filaments entering the suction inlet b. Filaments spiraling downward along the inner wall c. Filaments separating from the high-velocity airflow zone d. Filaments falling into the collection box

Figure 7 Motion trajectory of safflower filaments based on CFD-DEM coupling

integrates a vision perception system, a picking robotic arm system, a control system, a negative pressure collection system, and an end-effector module. It is capable of validating different picking point positioning algorithms, end-effector structural configurations, and the performance of the collection device. The negative pressure collection system consists of an RB-61D-A2 negative pressure fan (2.2 kW) and a Delta VFD022M+23B 2.2 kW frequency converter, allowing for the adjustment of the fan's operational state to conduct performance evaluation and comparison of harvesting effectiveness under different negative pressure conditions.

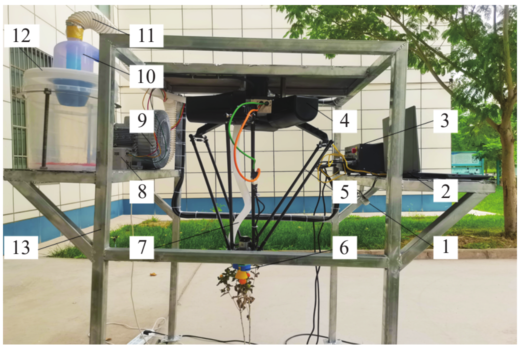

1. Intel Realsense D456 Camera 2. Host Computer Controller 3. Robotic Arm Control System 4. Drive Motor 5. Robotic Arm Link 6. End Effector 7. Conveyor Hose 8. VFD022M+23B Frequency Converter 9. RB-61D-A2 Fan 10. Cyclone Collection Device 11. Negative Pressure Duct 12. Collection Box 13. Frame

Figure 8 Safflower filament harvesting test platform

The material used in the tests was fresh safflower filaments harvested during the picking season. Before testing, the filaments were placed in a material tray, and their mass was weighed using a Lichen FA1204 electronic balance, recorded as m_0. During the tests, the fan airflow was controlled by adjusting the frequency converter. An M220M-16G high-speed camera was used to record the motion trajectory of the filaments inside the cyclone separation drum. The air velocity at the gathering inlet of the end-effector was measured using a DYL-1603 high-precision anemometer. Each test group was repeated five times, and the average value was taken to minimize random errors during operation. After the test, the safflower filaments in the collection box were removed and weighed, recorded as m_1. Based on preliminary tests and the theoretical simulation analysis above, the volute wrap angle (135-225°), separation drum diameter (130-150 mm), and negative pressure air velocity (2.2-2.6 m/s) were determined as the experimental factors. A three-factor, three-level Box-Behnken Response Surface Design was employed[27,28], with the parameter factor coding as listed in Table 5. The collection rate and impurity rate were used as evaluation indices. Their calculation equations are given below.

$$Y_1 = \frac{m_1}{m_0} \times 100\% \tag{12}$$

$$Y_2 = \frac{m_2}{m_1 + m_2} \times 100\% \tag{13}$$

where, Y_1 is the Collection rate, %; Y_2 is the Impurity rate, %; m_0 is the total mass of safflower filaments before collection, g; m_1 is the total mass of safflower filaments after collection, g; m_2 is the total mass of impurities after collection, g.

Table 5 Coding table for experimental factor levels

Coded level	Volute wrap angle A/(°)	Separation drum diameter B/mm	Negative pressure air velocity C/m·s^{-1}
–1	135	130	2.2
0	180	140	2.4
1	225	150	2.6

4.2 Test results and analysis

Tests were conducted according to the above method, and the results are listed in Table 6.

Table 6 Experimental design and results

No.	Experimental factors			Evaluation indicators	
	Volute wrap angle A/(°)	Separation drum diameter B/mm	Negative pressure air velocity C/m·s^{-1}	Collection rate Y_1/%	Impurity rate Y_2/%
1	–1	–1	0	97.12	2.65
2	1	–1	0	96.95	2.6
3	–1	1	0	97.34	2.62
4	1	1	0	97.08	2.53
5	–1	0	0	97.16	2.65
6	1	0	–1	97.13	2.68
7	–1	0	1	97.55	2.62
8	1	0	1	97.14	2.34
9	0	–1	–1	97.12	2.40
10	0	1	–1	97.65	2.48
11	0	–1	1	97.69	2.37
12	0	1	1	97.47	2.23
13	0	0	0	98.54	2.26
14	0	0	0	98.53	2.3
15	0	0	0	98.48	2.29
16	0	0	0	98.58	2.29
17	0	0	0	98.40	2.27

The experimental data from Table 6 were processed and analyzed using Design-Expert software (Design-Expert 12.0, Stat-Ease, Inc.). Regression variance models for the collection rate and impurity rate, considering the factors volute wrap angle A, separation drum diameter B, and negative pressure air velocity C, were obtained, as listed in Table 7.

Table 7 Regression variance models for safflower filament collection rate and impurity rate

Sources	Collection rate Y_1/%				Impurity rate Y_2/%			
	Sum of squares	*df*	*F*-value	*p*-value	Sum of squares	*df*	*F*-value	*p*-value
Model	5.95	9	239.22	<0.0001	0.43	9	87.49	<0.0001
A	0.095	1	34.24	0.0006	0.019	1	34.98	0.0006
B	0.054	1	19.70	0.0030	3.200E-3	1	5.89	0.0457
C	0.078	1	28.23	0.0011	0.053	1	97.16	<0.0001
AB	2.025E-3	1	0.73	0.4203	4.000E-4	1	0.74	0.4194
AC	0.036	1	13.06	0.0086	0.024	1	44.20	0.0003
BC	0.14	1	50.89	0.0002	0.012	1	22.26	0.0022
A^2	2.77	1	1000.86	<0.0001	0.29	1	524.64	<0.0001
B^2	1.38	1	500.24	<0.0001	0.014	1	25.83	<0.0001
C^2	0.85	1	309.21	<0.0001	3.853E-3	1	7.09	<0.0001
Residual	0.019	7			3.805E-3	7		
Lack of fit	2.250E-4	3	0.016	0.9969	2.725E-3	3	3.36	0.1359
Pure error	0.019	4			1.080E-3	4		
Cor total	5.97	16			0.43	16		

Note：p<0.01(extremely significant), 0.01≤p≤0.05 (significant).

As shown in Table 7, the regression models for both the collection rate and the impurity rate are extremely significant (p<0.0001). Specifically, for the collection rate (Y_1), factors *A* (volute wrap angle), *B* (separation drum diameter), *C* (negative pressure air velocity), the *AC* and *BC* interaction terms, and the quadratic terms A^2, B^2, C^2 have a highly significant influence, whereas the *AB* interaction is not significant. For the impurity rate (Y_2), factors *A*, *B*, the *AC* interaction, and the quadratic terms A^2, B^2, C^2 have a highly significant influence; factor *C* and the *BC* interaction have a significant influence; and the *AB* interaction is not significant for either response. The lack of fit p-values for the two models are 0.9969 and 0.1359, respectively, indicating that the experimental design is reasonable, the model fits well, and it adequately represents the relationship between the factors and the evaluation indicators. Based on the ANOVA results, non-significant terms were eliminated to obtain the simplified quadratic regression equations for collection rate (Y_1) and impurity rate (Y_2), shown as Equations (14) and (15), respectively.

$$Y_1 = 98.51 - 0.11A + 0.083B + 0.099C - 0.023AB - 0.095AC - 0.19BC - 0.81A^2 - 0.57B^2 - 0.45C^2 \tag{14}$$

$$Y_2 = 2.28 - 0.049A - 0.020B - 0.081C - 0.010AB - 0.078AC - 0.055BC + 0.26A^2 + 0.058B^2 + 0.030C^2 \tag{15}$$

Figure 9 presents the response surface analysis results for the factors affecting the collection rate. From Figure 9a, it can be observed that when the negative pressure air velocity is fixed at the central level (2.4 m/s), the collection rate exhibits a non-linear trend, first increasing and then decreasing, with increases in both the volute wrap angle and the separation drum diameter. This indicates the existence of a clear optimal parameter range. Contour analysis further identifies a high collection rate region (collection rate>98.3%) concentrated within a volute wrap angle range of 160°-197° and a separation drum diameter range of 135-145 mm. The volute wrap angle has a more pronounced effect on the collection rate, suggesting that geometric shape is the dominant factor determining flow separation efficiency. Figure 9b shows that when the separation drum diameter is fixed at 140 mm, the collection rate exhibits a monotonically decreasing trend as the volute wrap angle increases, indicating that an excessively large wrap angle may lead to a decay in airflow rotational intensity, which is detrimental to the effective capture of filaments. Simultaneously, the collection rate remains high within the ranges of 160°-205° for the volute wrap angle and 2.3-2.5 m/s for the negative pressure air velocity, further confirming the volute wrap angle as the most critical influencing factor. Figure 9c further indicates that when the volute wrap angle is fixed at 180°, the collection rate gradually decreases as the separation drum diameter increases, suggesting that a smaller drum diameter helps enhance the centrifugal force field and improves collection performance. Comprehensive analysis reveals that the influence of structural parameters (wrap angle and drum diameter) on the collection rate is greater than that of the operational parameter (air velocity), highlighting the importance of structural optimization in enhancing collection efficiency.

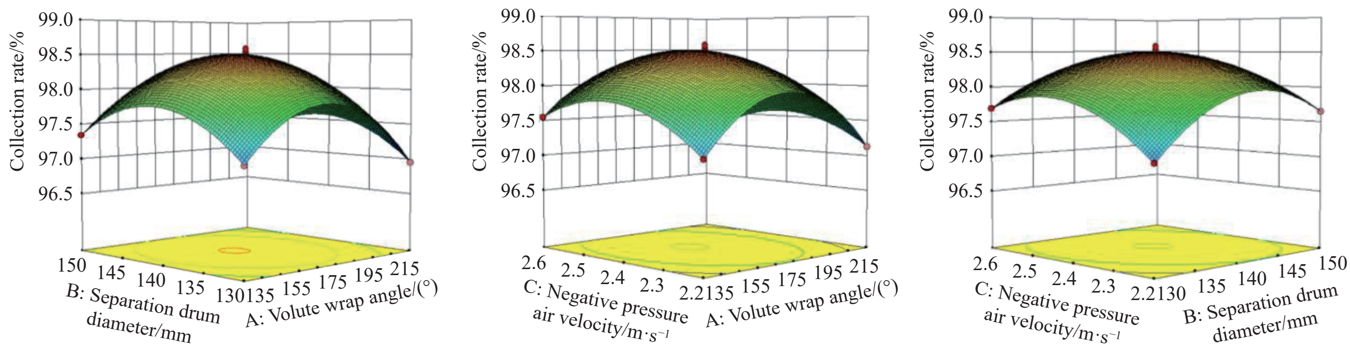

a. $Y_1=f(A,B)$ b. $Y_1=f(A,C)$ c. $Y_1=f(B,C)$

Figure 9 3D surface plots showing the effects of different factors on the collection rate

Figure 10 presents the response surface analysis results for the factors affecting the impurity rate. From Figure 10a, it can be seen that when the negative pressure air velocity is fixed at the central level (2.4 m/s), the impurity rate first decreases and then increases with increases in both the volute wrap angle and the separation drum diameter, indicating that optimal values exist for both parameters that minimize the impurity rate. Specifically, within the parameter ranges of 170°-195° for the volute wrap angle and 135-145 mm for the separation drum diameter, the impurity rate can be maintained at a low level (<2.4%), indicating that this structural configuration can effectively enhance impurity separation efficiency. Figure 10b further shows that when the separation drum diameter is fixed at 140 mm, the impurity rate also demonstrates a non-linear relationship, first decreasing and then increasing, with an increase in the volute wrap angle, while it continuously decreases with an increase in air velocity. This suggests that increasing the air velocity within a certain range helps enhance the impurity removal capability. Figure 10c indicates that when the volute wrap angle is fixed at 180°, the impurity rate shows a monotonically increasing trend as the separation drum diameter increases, suggesting that a smaller drum diameter favors enhanced impurity separation by strengthening the centrifugal force field. Comprehensive analysis of the response surfaces indicates that the influence of structural parameters (volute wrap angle and separation drum diameter) on the impurity rate is significantly greater than that of the operational parameter (negative pressure air velocity), underscoring the dominant role of structural optimization in controlling the impurity rate.

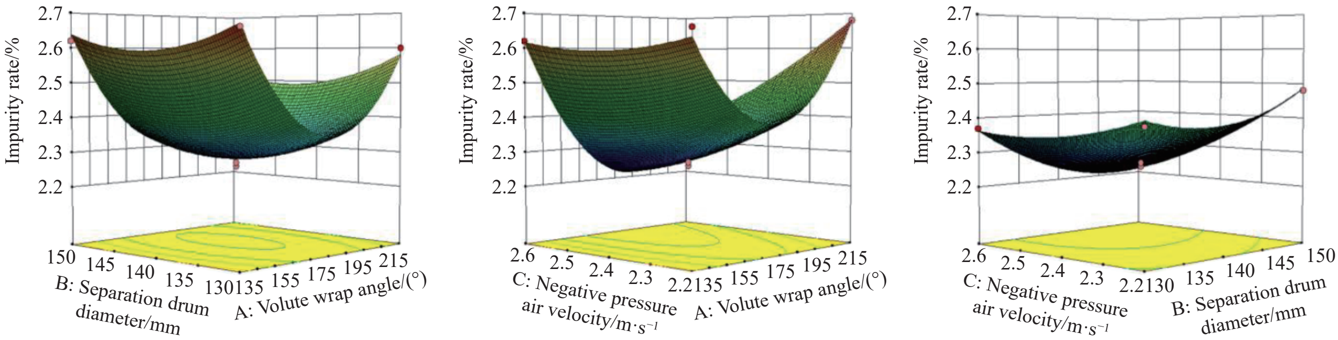

a. $Y_2=f(A,B)$ b. $Y_2=f(A,C)$ c. $Y_2=f(B,C)$

Figure 10 3D surface plots showing the effects of different factors on the impurity rate

4.3 Parameter optimization and experimental verification

To achieve the optimal operating parameters for the cyclone separator's cleaning performance, an optimization solution for the influencing factors was performed using the Optimization-Numerical module in Design-Expert 12.0, based on safflower filament harvesting requirements and the aforementioned analysis results. The objective function and constraints are shown in Equation (16)[29]. The optimal parameter combination was obtained as: volute wrap angle of 181.668°, separation drum diameter of 141.005 mm, and negative pressure air velocity of 2.470 85 m/s. Under these conditions, the predicted filament collection rate was 98.4738%, and the predicted impurity rate was 2.251 12%.

$$\begin{cases} \max Y_1 = f(A,B,C) \\ \min Y_2 = f(A,B,C) \\ \text{s.t.} \begin{cases} 135^\circ \le A \le 225^\circ \\ 130\ \text{mm} \le B \le 145\ \text{mm} \\ 2.2\ \text{m/s} \le C \le 2.6\ \text{m/s} \end{cases} \end{cases} \tag{16}$$

To further verify the reliability of the optimized parameters, the values were rounded to a volute wrap angle of 180°, a separation drum diameter of 140 mm, and a negative pressure air velocity of 2.5 m/s for repetitive validation tests, as shown in Figure 11.

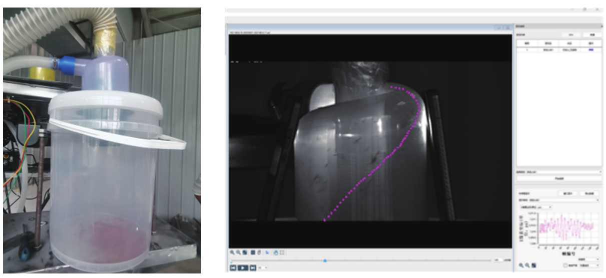

a. Collection process b. High-speed camera motion trajectory

Figure 11 Safflower filament collection test

The safflower filament collection process and the motion trajectory inside the separation drum are shown in Figure 11. The trajectory captured by high-speed camera technology indicates that filaments entering the separation drum swirl approximately half a revolution along the inner wall under the action of the airflow before successfully falling into the collection box. Through five repeated tests, the average collection rate was 98.53%, and the average impurity rate was 2.3%, meeting the requirements for safflower filament harvesting operations. This effectively validates the correctness of the previous theoretical analysis.

5 Discussion

Aiming at the difficulty of mechanized collection of safflower filaments after picking, this paper designed a cyclone separation cleaning and collection device for safflower filaments based on gas-solid two-phase flow theory. The key structural parameters (volute wrap angle, separation drum diameter) of the cyclone separator were numerically simulated and optimized using Fluent software. Subsequently, the Fluent-EDEM coupling method was employed to systematically optimize its operational parameters, thereby determining the optimal parameter combination. To verify the reliability of the numerical simulation results, a test bench was built, and tests under actual working conditions were conducted, obtaining key performance indicators: the filament collection rate and the impurity rate. Design-Expert 12.0 software was further used to process the experimental data, establishing regression models for the filament collection rate and the impurity rate, and the influence of various factors on their performance was compared and discussed. Based on response surface analysis, the interaction effects between the three key factors on the collection rate and the impurity rate were systematically evaluated. Finally, multi-objective parameter optimization was carried out using the Optimization module in Design-Expert, yielding the optimal parameter combination: volute wrap angle of 180°, separation drum diameter of 140 mm, and negative pressure air velocity of 2.5 m/s. Test results under this combination showed a filament collection rate of 98.53% and an impurity rate of 2.3%, which are in high agreement with the model predictions, indicating that the established model has significant guiding importance for optimizing the filament cleaning process. However, this study still has certain limitations:

(1) During the optimization process, the focus was on the main structural parameters and operational parameters of the cyclone separator, without considering the potential impact of the plunger tube's aperture size and its positioning on cleaning performance. Although this strategy reduced experimental complexity and cost to some extent, plunger tube blockage might occur during the cleaning process of high-concentration safflower materials due to structural

mismatch, thereby affecting the continuous operational efficiency of the device.

(2) The research focused on the influence of the volute wrap angle and separation drum diameter on the internal flow field characteristics and cleaning effect, and did not investigate the potential impact of the discharge outlet structure (such as the exit curvature) on the internal flow field structure and performance. Although simplifying structural variables helps control the experimental scale, further exploration of the influence of the discharge outlet curvature on airflow organization and material motion trajectory is expected to further improve the comprehensive cleaning performance of the cyclone separator.

Future work will focus on researching the internal flow field mechanism based on gas-solid two-phase flow theory to reveal the motion patterns of different materials within the flow field, aiming to expand the cleaning device's adaptability to various crops. Furthermore, we plan to integrate an intelligent control system with the cleaning device to achieve dynamic optimization of the internal flow field through real-time monitoring and feedback regulation, thereby enhancing the operational stability and cleaning efficiency of the device under different working conditions.

6 Conclusions

(1) Aiming to address the technical challenge of the lack of efficient cleaning equipment for safflower filaments, this study proposed and developed a safflower filament cleaning system based on the cyclone separation principle. The system consists of core modules including an end-effector, conveying hose, cyclone collector, negative pressure fan, and collection box. Focusing on the core component—the cyclone collector—the study preliminarily determined its structural parameters based on gas-solid two-phase flow theory.

(2) To enhance the performance of the cyclone collector, numerical simulation using Fluent fluid dynamics based on the RNG k-ε turbulence model was conducted. Taking the volute wrap angle and the separation drum diameter as key structural parameters, in-depth analysis and optimization were performed from the aspects of pressure contours, velocity contours, and particle trajectories, determining the optimal ranges for the volute wrap angle and the separation drum diameter of the cyclone collector. Based on the principles of low energy consumption, low damage, and high efficiency, simulation analysis determined the optimal range for the operational parameter, the negative pressure air velocity. Furthermore, a CFD-DEM gas-solid coupling numerical simulation method was adopted to systematically optimize the performance of the cyclone collector under different working conditions. Simulation results indicated that under the optimal operating parameter range, the theoretical damage rate of filaments could be controlled at 2.5%.

(3) To verify the simulation results and the actual performance of the system, a safflower filament harvesting performance test platform was established, validating the filament collection rate and the impurity rate under different working conditions. Design-Expert 12.0 software was primarily used for statistical analysis of the platform test data, establishing variance regression models for the filament collection rate and the impurity rate against various influencing factors. By analyzing the variance regression models, the interaction between factors and their contribution to the performance indicators were clarified. Using the software's multi-objective optimization module Optimization-Numerical, the global optimal parameter combination was determined: volute wrap angle of 181.668°, separation drum diameter of 141.005 mm, and negative pressure air velocity of 2.470 85 m/s. Under this configuration, the model predicted a filament collection rate of 98.47% and an impurity rate of 2.25%. Considering practical operation, the optimized parameters were rounded to a volute wrap angle of 180°, a separation drum diameter of 140 mm, and a negative pressure air velocity of 2.5 m/s for repetitive validation tests. The results showed a filament collection rate of 98.53% and an impurity rate of 2.30%. The experimental results demonstrate that the relative errors of all key indicators compared to the predicted values are less than 5%. This research provides a new solution for safflower filament cleaning technology and offers effective theoretical support and a practical basis for the design and performance optimization of cyclone collectors.

Acknowledgements

This research was funded by the Natural Science Foundation of Xinjiang (Grant No. 2025D01C89), National Natural Science Foundation of China (NSFC) (Grant No. 32560422), and the second batch of Tianshan Talent Cultivation Plan for Young Talent Support Project (Grant No. 2023TSYCQNTJ0040).

[References]

[1] National Pharmacopoeia Commission. Pharmacopoeia of the People's Republic of China, Part I. China Medical Science Press, 2020. (in Chinese)

[2] Wang X, Shang J Y, Hui J, Zhao J K, Wang X Y, Wang L M, et al. Research progress on nutrients and efficacy of safflower seed oil. China Oils Fats, 2024; 10: 66–71. (in Chinese)

[3] Ge Y, Zhang L X, Gu J W, Fu W, Fu R G, Zhang H M. Parameter optimization and experiment of dual roller harvesting device for safflower. Transactions of the CSAE, 2015; 31(21): 35–42. (in Chinese)

[4] Zhang Z G, Xing Z Y, Yang S P, Feng N, Liang R Q, Zhao M Y. Design and experiments of the circular arc progressive type harvester for the safflower filaments. Transactions of the CSAE, 2022; 38(17): 10–21. (in Chinese)

[5] Zhang X W, Ge Y, Zhang L X, Chen F, Ma W X. Design and experiment of rectangular safflower picking robot. J. Agricultural Mechanization Research, 2022; 44(1): 79–84. (in Chinese)

[6] Cao W B, Lian G D, Niu C, An L L, Yang S P, Chen B B. Harvest performance test and parameter optimization of comb-type safflower-filaments picking head at same height. Transactions of the CSAE, 2018; 34(22): 36–44. (in Chinese)

[7] An L L, Cao W B, Li S F, Ma P, Lian G D, Yang S P. Design of hydraulic system for comb-clamping safflower harvesting machine. J. Chinese Agricultural Mechanization, 2020; 41(1): 37–42. (in Chinese)

[8] Yang M, Hu Z, Zhang Y, Xu H, Gu F, Wu F. Research status and prospect of pneumatic cleaning device for agricultural granular materials. J. China Agricultural Mechanization, 2020; 41(3): 121–127. (in Chinese)

[9] Liao Q X, Wan X Y, Li H T, Ji M Y, Wang H. Design and experiment on cyclone separating cleaning system for rape combine harvester. Transactions of the CSAE, 2015; 31(14): 24–31. (in Chinese)

[10] Huang Y S, Zhang W G, Feng S K, Liu Z J, Yang F Z. Buckwheat cyclone separation and cleaning device based on EDEM-Fluent. J. Northwest A&F Univ., 2023; 51(10): 128–140. (in Chinese)

[11] Wasilewski M, Singh L, Ligus G. Experimental and numerical investigation on the performance of square cyclones with different vortex finder configurations. Sep. Purif. Technol., 2020; 239: 10–24.

[12] Baltrenas P, Pranskevicius M, Venslovas A. Optimization of the new generation multichannel cyclone cleaning efficiency. Energy Procedia, 2015; 72: 188–195.

[13] Brar L S, Elsayed K. Analysis and optimization of multi-inlet gas cyclones using large eddy simulation and artificial neural network. Powder Technol., 2017; 311: 465–483.

[14] Juengcharoensukying J, Poochinda K, Chalermsinsuwan B. Effects of cyclone vortex finder and inlet angle on solid separation using CFD simulation. Energy Procedia, 2017; 138: 1116–1121.

[15] Han D, Zhang D, Jing H, Li Y, Tao C, Ding Y, Wang Z, Wang Y, Zhang

T. DEM-CFD coupling simulation and optimization of an inside-filling air-blowing maize precision seed-metering device. Comput. Electron. Agric., 2018; 150: 426–438.

[16] Wu N, He J L, Liu S H, He Y Q. Simulation and experiment of air screen cleaning device for Cerasus humilis based on EDEM-Fluent coupling. Agricultural Engineering, 2021; 11(1): 82–87. (in Chinese)

[17] Wasilewski M. Analysis of the effect of counter-cone location on cyclone separator efficiency. Sep. Purif. Technol., 2017; 179: 236–247.

[18] Huang A N, Ito K, Fukasawa T, Fukui K, Kuo H P. Effects of particle mass loading on the hydrodynamics and separation efficiency of a cyclone separator. J. Taiwan Inst. Chem. Eng., 2018; 90: 61–67.

[19] Li X P, Meng Y J, Zhang J L, Geng L X, Ji J T. Design and test of cleaning device for roller rubbing cylinder sieve of millet. Transactions of the CSAM, 2018; 49(10): 92–102, 136. (in Chinese)

[20] Wang H H, Li Y M, Xu L Z, Huang M S, Ma Z. Simulation and experiment of air flow field in the cleaning device of ratooning rice combine harvesters. Transactions of the CSAE, 2020; 36(20): 84–92. (in Chinese)

[21] Hou J M, Ren Z T, Zhu H J. Design and test of double-layer inclined vibrating air-screen castor cleaning device. Transactions of the CSAM, 2022; 53(S2): 39–51.

[22] Chen Y, He J W, Yu X, Hu B, Li L H, Zhang X L, Liu X C, Mao R N. Design and experiment of air-suction roller corn precision dibbler based on DEM-CFD coupling. Int J Agric & Biol Eng, 2025; 18(5): 142–153.

[23] Xu H B, Zhang P, Gu F W, Hu Z C, Yang H G, Mao E R, Du Y F. Numerical simulation and experiment of dust suppression device of peanut whole-feed combine using computational fluid dynamics. Agriculture, 2023; 13(2): 329.

[24] Jiang T, Zhang M, Guan Z H, Mu S L, Wu C Y, Wang G, Li H T. Simulation and analysis of the pneumatic recovery for side-cutting loss of combine harvesters with CFD-DEM coupling approach. Int J Agric & Biol Eng, 2022; 15(2): 117–126.

[25] Sun X P, Li H, Qi X D, Feng D H, Zhou J Q, Wang Y J, Nyambura S M, Zhang X Y, Chen X. Optimization of a three-row air-suction Brassica Chinensis precision metering device based on CFD-DEM coupling simulation. Int J Agric & Biol Eng, 2023; 16(3): 130–142.

[26] Xu H M, Liu W R, Liu H, Liu Z F, Zhang G Z. Design and performance test of a combined and adjustable precise rice seed metering device. Int J Agric & Biol Eng, 2025; 18(1): 101–114.

[27] Chen J N, Li H, Liu L M, Jia J M, Zhao R M, Wu C Y. Design and experimental optimization of end effector for picking famous tea with split-cutter. Transactions of the CSAM, 2024; 55(1): 39–46, 195. (in Chinese)

[28] Shu C X, Yang J, Wan X Y, Yuan J C, Liao Y T, Liao Q X. Calibration and experiment of the discrete element simulation parameters of rape threshing mixture in combine harvester. Transactions of the CSAE, 2022; 38(9): 34–43. (in Chinese)

[29] Chen W H, Fei J M, Gao J P, Kan Z, Huang L D, Meng H W, Qi J T. Design and experiment of the traction tiger nut combine harvester. Int J Agric & Biol Eng, 2026; 19(2): 139–151.